Enhanced long-wavelength transient photoresponsiveness of WO_3 induced by tellurium doping

Bin Yang[ab] and Vittorio Luca*[ab]

Received (in Cambridge, UK) 6th May 2008, Accepted 10th June 2008
First published as an Advance Article on the web 29th July 2008
DOI: 10.1039/b807629d

Tungsten trioxide (WO_3) films doped with 0.25 atom% tellurium synthesised by a sol–gel route, show strong transient photocurrents under chopped sub-bandgap illumination ($h\nu = 1.8$ eV $< E_g$) at low bias potentials from 0.2 to 0.7 V; such effects are ascribed to the presence of a localized narrow band (NB) between the VB and the CB in this material.

Tungsten trioxide (WO_3) thin films have a wide range of applications due to their gas sensing,[1,2] electrochromic[3,4] and photocatalytic[5] properties. Such films are also promising electrode materials for the photoelectrochemical oxidation of water to produce hydrogen.[6–11] However, the energy conversion efficiencies of such films are generally low; mainly because the band gap of crystalline WO_3 is $E_g = 2.6$ eV which places limits on absorption of solar radiation. In order to modify the band gap, and modify light absorption properties, different elements were doped into WO_3 films. It was observed that tellurium-doping induced unique photoelectro-chemical properties. In this communication we report: (1) the synthesis of tellurium doped WO_3 films (2) the photoelectrochemical properties of the films and (3) a proposed bandgap model of the films.

The WO_3 films in this study were synthesized through a simple sol–gel route from peroxopolytungstic acid (PPTA) as previously described.[10] Briefly, the doped films were prepared in the following manner: a solution of 1.8 g of tungsten powder (Aldrich, 99.9%) dissolved in 60 mL of 30% hydrogen peroxide was combined in an appropriate ratio with a solution of 1.3 g of tellurium metal powder (Aldrich, 99.9%) dissolved in 50 mL of 30% hydrogen peroxide. Excess hydrogen peroxide in the resulting solution was decomposed using platinum black (Aldrich Chem. Co). This solution was diluted by adding the same volume of 2-propanol. Films were prepared by drop-casting the precursor tungstate solutions onto fluorine-doped tin oxide conducting glass substrates at room temperature followed by drying at 60 °C and annealing at 500 °C in air for 30 min. A series of samples with different doping ratios were prepared and characterized. We report here on two particular preparations: film A was a Te-doped film with a molar Te/W ratio of 0.0025 and film B was the undoped WO_3 film. Both films had comparable thickness of 5 μm.

[a] *Inst. of Materials Eng., Australian Nuclear Science and Technology Organisation, PMB 1, Menai, NSW 2234, Australia. E-mail: vlu@ansto.gov.au; Fax: +61 2 9717 9630; Tel: +61 2 9717 9563*
[b] *CSIRO National Hydrogen Materials Alliance, CSIRO Energy Centre, 10 Murray Dwyer Circuit, Steel River Estate, Mayfield West, NSW 2304, Australia*

The photoelectrochemical properties of the films were investigated using a VoltaLab model PGZ 402 potentiostat with a three electrode configuration comprising the WO_3 working electrode, a platinum wire counter electrode and an Ag/AgCl reference electrode. In all cases aqueous solutions of 1 M H_2SO_4 were used as the electrolyte. The working electrode was illuminated by a 1000 W Oriel 6271 ozone-free xenon lamp with light density of 86 mW cm^{-2}. Incident Photon Conversion Efficiency (IPCE) values were recorded using a lock-in amplifier. A monochromator and a chopper were set between the light source and the working electrode.

Fig. 1 shows potentiodynamic scans of (a) film A under chopped red light ($h\nu = 1.8$ eV $< E_g$), (b) film A under chopped white light, (c) film B under chopped red light and (d) film B under chopped white light. Curve (a) indicates clearly that film A had a significant response to red light with the

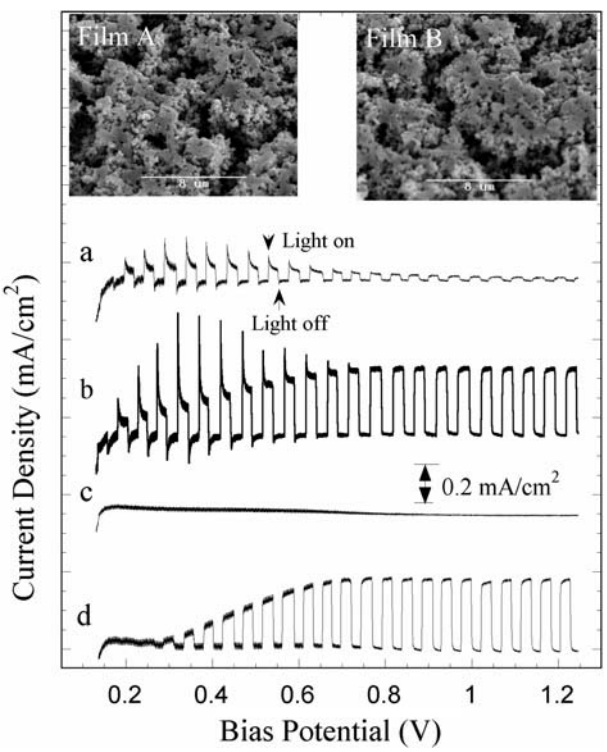

Fig. 1 Potentiodynamic scans of (a) film A under chopped red light (sub-bandgap illumination, $h\nu = 1.8$ eV); (b) film A under chopped white light; (c) film B under chopped red light; and (d) film B under chopped white light. The SEM images films A and B are inserted no the top of this figure, show that the texture of the two films are same.

presence of both a transient spike and a quasi steady-state photocurrent in the potential range between 0.15 and 0.7 V. When the potential was higher than 0.7 V a weak steady-state photocurrent persisted. In comparison, film B showed no photoresponse to red light, as shown in curve (c). Under white light, film A generated an intense transient photocurrent with a maximum peak value of 0.4 mA cm^{-2}, in the potential range between 0.15 and 0.7 V, while curve (d) showed that a stationary photocurrent was generated by film B. Comparing (b) and (d), the photocurrent onset was displaced to lower potentials for the Te-doped film. The inset to Fig. 1 shows that doping has no significant impact on the open porous morphology of the films.

Fig. 2 shows incident photon conversion efficiency (IPCE) curves of (a) film A under 40 Hz chopped illumination at bias potential of 0.4 V, (b) film A at 160 Hz and 0.4 V bias, (c) film B at 40 Hz and 0.4 V bias and (d) film A at 40 Hz at 1.0 V bias. Curves (a) and (b) demonstrate that film A responded to a wide range of light wavelengths from 300 (ultraviolet) to 800 nm (near infrared) at a bias potential of 0.4 V. In particular, in the short wavelength region ($\lambda < 430$ nm), the signal was similar to that of a conventional IPCE curve for a pure WO_3 film;[9] characterised by the presence of a peak at 400 nm. In contrast, for $\lambda > 430$ nm, the intensity of the signal decayed exponentially as $e^{-0.014\lambda}$. Moreover, we note that curve (a) has a higher IPCE value than (b), which indicates that photoresponse decreased as the chopping frequency rose. In comparison, the photoresponse for the undoped film shown in curve (c) decreased rapidly with an onset at approximately 460 nm. This is similar to the IPCE curve of pure crystalline WO_3.[9] Comparing (a) and (c), the photocurrent from film A was much higher than that of film B under the same conditions. This indicates that the transient photoresponse is much stronger than the steady-state photoresponse at a bias of 0.4 V. Comparing (a) and (d), it is interesting to note the absence of a long wavelength photoresponse of film A at the higher

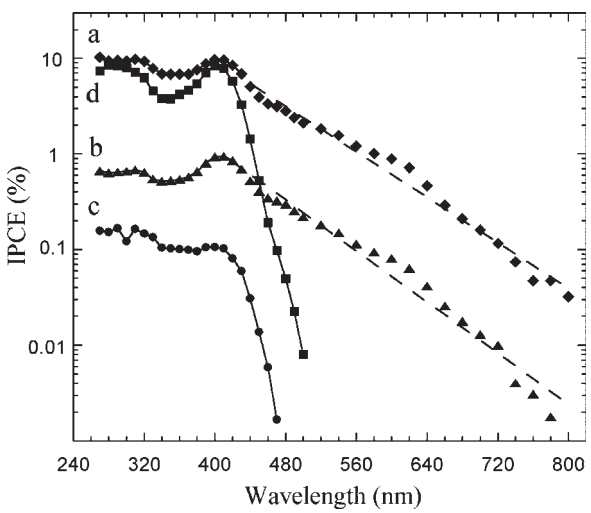

Fig. 2 IPCE curves recorded at bias potential of 0.4 V of (a) film A under a 40 Hz chopped illumination; (b) film A at 160 Hz; and (c) film B at 40 Hz. (d) The IPCE curve of film A at bias potential of 1.0 V under a 40 Hz chopped illumination. The dashed lines have the form $e^{-0.014\lambda}$.

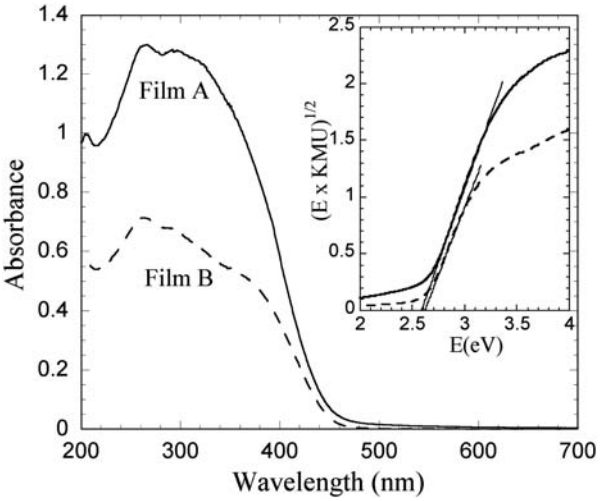

Fig. 3 UV-Vis absorption spectra of film A and B with the Tauc plot in the inset.

bias potential of 1 V. This agrees with the experimental data in Fig. 1(b), in which the transient spikes appeared only at bias potentials lower that 0.7 eV, and confirms the absence of transient photocurrents at higher potentials.

Optical absorption spectra of the films were measured using a Cary 500 UV-Vis spectra equipped with a diffuse reflectance accessory. Fig. 3 shows the absorption spectra of films A and B with the absorption onset at about 480 nm. The bandgap values were determined using a Tauc plot which shows $(h\nu \times \mathrm{KMU})^{1/2}$ *vs.* $h\nu$ where $h\nu$ and KMU are photon energy and Kubelka–Munk units of absorption, respectively (see Fig. 4 inset). The plot of Fig. 3 shows that the band gaps of the doped and undoped WO_3 films are similar and about 2.6 eV, indicating that the doping of Te has very little influence on the absorption onset. However, there are two notable differences between the films. First, the absorption edge of film A had about 40% greater intensity than that of film B and had different fine structure around 300 nm. Second, the absorption edge of film A displayed a low intensity absorbance tail extending to long wavelength. This tail is similar to the Urbach tail of TiO_2,[12] and in similar fashion is likely to be caused by impurities, lattice disorder and the localized state excitations in the material.

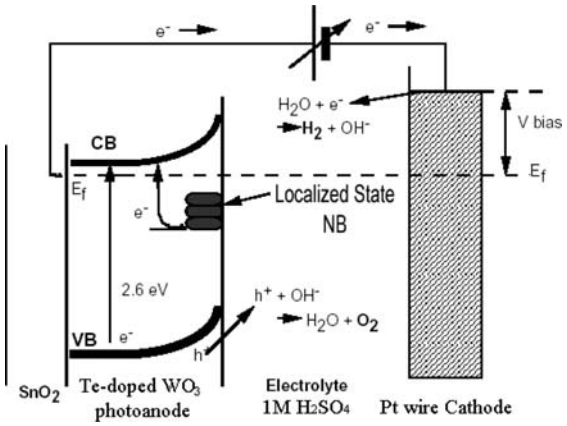

Fig. 4 Model of band structure of film A in the electrolyte.

We believe that these pronounced differences in the fundamental absorption edges of the doped and undoped films itself provides indirect evidence that Te atoms are really incorporated into the bulk or near surface structure of the WO_3 nanoparticles. In previous studies of undoped WO_3 nanoparticle materials by our group we have not observed any such dramatic variations in the optical absorption edges as a function of variation in texture.[10] This further supports the notion that the observed modifications to the optical properties are most likely explained by a genuine doping. In addition, the X-ray diffraction pattern of the Te-doped WO_3 film with an atomic Te/W ratio up to 1/100 was identical to that of pure WO_3. The fact that there was no measurable change in particle size indicates that the crystalline lattice of WO_3 was not affected by doping. Hence, it is reasonable to expect that the presence of Te atoms in bulk or near surface of the WO_3 nanoparticles may result in the creation of localized sub-bandgap states and play an important role in producing the transient photocurrents.[13]

In order to explain the dramatic photoresponse upon sub-bandgap illumination observed in this work, a model of the band structure of the Te doped WO_3 is proposed in Fig. 4. Similar to the bandgap structure suggested by Preusser *et al.*,[14] we assume that doping of Te creates a set of narrow bands (NB) of localized electronic states located between VB and CB. The NB can be filled or emptied rapidly as the Fermi level (E_f) passes through the states. Here, as shown in Fig. 5, the photoresponse of film A under two different cases is considered. The first case is when E_f is higher than NB and NB is filled. The second case is when E_f is lower than NB and NB is empty. In the first case, when the film is suddenly illuminated by super-bandgap photons ($h\nu > E_g = 2.6$ eV), CB receives photo excited electrons from both VB and NB and contributes to the quasi steady state and transient photocurrent, respectively. When the light is switched off, electrons fall back to NB, and a negative spike appears. If we substitute super-bandgap illumination by sub-bandgap illumination ($h\nu < E_g$), CB can only receive electrons from NB and generates a transient photocurrent. A stationary photocurrent can not be generated because E_g is not high enough to pump electrons from VB. This case corresponds to the potential from 0.2 to 0.75 V. The photoresponse is shown in Fig. 1(b) and (a), respectively. In the second case, it corresponds to a potential bias greater than 0.8 V. When the film is illuminated by super-bandgap photons, only a stationary photocurrent can be generated, because the NB is empty. This is good agreement with the experimental observations shown in Fig. 1(b) (from 0.8 to 1.2 V). When the film is illuminated by sub-bandgap light it is expected that there will be absence of both stationary and transient photocurrents. However, a small quasi-stationary photocurrent was also displayed experimentally. This is shown in Fig. 1(a) at bias potentials greater than 0.8 V. This could be induced by either the presence of residual electrons in the NB or by a two-step excitation mechanism; electrons pumped up from VB to NB and then from NB to CB.

In conclusion, Te-doped WO_3 films show interesting and unique photoelectrochemical properties generating strong transient photocurrents under sub-bandgap illumination and enhanced photoresponses at longer wavelengths. Such effects are induced by the incorporation of Te atoms into the bulk or surface structure of the WO_3 nanoparticles, resulting in a modification of the band structure. While further detailed investigation of the reported phenomena are under way, the present novel doping strategy may pave the way to electrode materials with enhanced performance in the photoelectrolysis of water.

The authors are grateful to Dr Piers R. F. Barnes of CSIRO, Industrial Physics, and Dr Yingjie Zhang of ANSTO for his assistance in acquiring photoresponse and absorption data for the films.

Notes and references

1 C. Cantalini, L. M. Lozzi, S. Passacantando and Santucci, *IEEE Sens. J.*, 2003, **3**, 171.
2 J. Tamaki, Y. Okochi and S. Konishi, *Electrochemistry*, 2006, **74**, 159.
3 M. Deepa, R. Sharma, A. Basu and S. A. Agnihotry, *Electrochim. Acta*, 2005, **50**, 3545.
4 W. Cheng, E. Baudrin, B. Dunn and J. I. Zink, *J. Mater. Chem.*, 2001, **11**, 92.
5 H. Habazaki, Y. Hayashi and H. Konno, *Electrochim. Acta*, 2002, **47**, 4181.
6 A. Fujishima and K. Honda, *Nature*, 1972, **238**, 37.
7 B. Yang, H. J. Li, M. Blackford and V. Luca, *Curr. Appl. Phys.*, 2006, **6**, 436.
8 W. Erbs, J. Desilvestro, E. Borgarello and M. Gratzel, *J. Phys. Chem.*, 1984, **88**, 4001.
9 C. Santato, M. Odziemkowski, M. Ulmann and J. Augustynski, *J. Am. Chem. Soc.*, 2001, **123**, 10639.
10 B. Yang, P. R. F. Barnes, W. Bertram and V. Luca, *J. Mater. Chem.*, 2007, **17**, 2722.
11 S. H. Baeck, T. Jaramillo, G. D. Stucky and E. W. McFarland, *Nano Lett.*, 2002, **2**, 831.
12 H. Tang, F. Levy, H. Berger and P. E. Schmid, *Phys. Rev. B*, 1995, **52**, 7771.
13 L. M. Peter, *Chem. Rev.*, 1990, **90**, 753.
14 S. Preusser, U. Stimming and S. Tokunaga, *J. Electrochem. Soc.*, 1995, **142**, 102.

